Monolithic Liquid Crystal Waveguide Fourier Transform Spectrometer for Gas Species Sensing

Tien-Hsin Chao, Thomas T. Lu,
Jet Propulsion Laboratory
4800 Oak Grove Drive, Pasadena CA, 91109

Scott R. Davis, Scott D. Rommel, George Farca, Ben Luey, Alan Martin, Michael H. Anderson
Vescent Photonics Inc.
4865 E. 41st Ave, Denver CO, 80216

Key Words: Solid-state Fourier transform spectrometer, liquid crystal clad waveguide, monolithic spectrometer, near-IR spectrometer, electro-optic FTIR

ABSTRACT

Jet Propulsion Lab and Vescent Photonics Inc. and are jointly developing an innovative ultra-compact (volume < 10 cm^3), ultra-low power (<10^{-3} Watt-hours per measurement and zero power consumption when not measuring), completely non-mechanical Liquid Crystal Waveguide Fourier Transform Spectrometer (LCWFTS) that will be suitable for a variety of remote-platform, in-situ measurements. These devices are made possible by novel electro-evanescent waveguide architecture, enabling "monolithic chip-scale" Electro Optic-FTS (EO-FTS) sensors. The potential performance of these EO-FTS sensors include: i) a spectral range throughout 0.4-5 μm (25000 – 2000 cm^{-1}), ii) high-resolution ($\Delta\lambda \leq 0.1$ nm), iii) high-speed (< 1 ms) measurements, and iv) rugged integrated optical construction. This performance potential enables the detection and quantification of a large number of different atmospheric gases simultaneously in the same air mass and the rugged construction will enable deployment on previously inaccessible platforms. The sensor construction is also amenable for analyzing aqueous samples on remote floating or submerged platforms. We will report a proof-of-principle prototype LCWFTS sensor that has been demonstrated in the near-IR (range of 1450-1700 nm) with a 5 nm resolution. This performance is in good agreement with theoretical models, which are being used to design and build the next generation LCWFTS devices.

1. INTRODUCTION

Traditional Fourier transform spectrometers possess two major advantages over grating, prism, and circular variable filter (CVF) spectrometers. One is the time-multiplexing effect. The Michelson interferometer's single detector views all the wavelengths (within the sensor passband) simultaneously throughout the entire measurement. This effectively lets the detector collect data on each wavelength for the entire measurement time, measuring more photons and therefore, results in higher signal-to-noise ratio, at best for situations where the source is stable. The other is the throughout advantages since the FTS does not need spatial filters (e.g. slit) in the optical light path.

However, traditional FTIR spectrometers, used in flight missions, obtain their optical delay by physically translating one or more optical components. This translation mechanism dominates the risk, cost, power consumption, and performance of such instruments because:

- Over the course of a 5-year mission, tens of millions of strokes will be required, making wear or fatigue a serious risk

Optical Pattern Recognition XXII, edited by David P. Casasent, Tien-Hsin Chao, Proc. of SPIE Vol. 8055
805506 · © 2011 SPIE · CCC code: 0277-786X/11/$18 · doi: 10.1117/12.886146

- The moving optical element cannot be rigidly held, making it sensitive to vibration and requiring that it be "caged" during launch to prevent damage, adding risk (failure of the caging mechanism to reopen)
- Accelerating and decelerating the optical elements can torque the spacecraft, making it difficult to maintain accurate pointing.

A high-resolution FTIR spectrometer without moving parts therefore represents a substantial improvement in reliability, mission duration, and performance. It also promises to be much smaller in size and mass and less power consumptive.

We have been developing a compact LCWFTS sensor with the following performance features: ultra-compact (volume < 10 cm^3), ultra-low power (<10^{-3} Watt-hours per measurement and zero power consumption when not measuring), completely non-mechanical electro-optic Fourier transform spectrometer (E-O FTS), operating at the near IR near-IR (range of 1450-1700 nm) utilizing an electro-evanescent liquid crystal (LC)-waveguide architecture.

FTIR (Fourier Transform Infrared) spectroscopy has been established as a powerful tool for measurements of atmospheric trace gases. Using the sun or moon as light source, between 20-30 trace gases of the tropo- and stratosphere can be detected and qualified from their absorption features.

This LCWFTS consists of: i) a unique LC-waveguide architecture as the solid-state time delay device whose optical path difference (OPD) can be precisely varied utilizing voltage control, ii) a photodetector diode, and iii) an external light/sample collecting devices tailored for either in-situ gas and/or rock sample analysis or for remote atmospheric gas analysis. In operation, letting the light beams pass through the LC cladded waveguide generates a time delay with respect to each wavelength. This time delay can be precisely controlled by controlling the voltage applied. This innovative E-O scanning scheme enables precise time delay data similar to that obtained by a conventional mechanical FTS that uses a Michelson interferometer. However, by eliminating all moving parts, the proposed E-O FTS will be less fragile with much higher reliability and durability.

The LCWFTS, upon full construction, will result in over 3 orders of magnitude reduction in mass, volume, power, and telemetry rate relative to existing Fourier transform Spectrometers such as the Fourier Transform Infrared (FTIR, widely deployed for Earth Orbiting observation missions) , Mini-Thermal Emission Spectrometer (Mini-TES, to be deployed with Athena Mars exploration rovers) instrumentation. This sensor will operate at a spectral range throughout 0.4 -5 μm (25000 – 2000 cm^{-1}, thereby allowing high-resolution, high-speed measurement of a large number of different atmospheric gases simultaneously in the same airmass. This unique capability meets those required by both the NASA Mars Exploration Program (MEP) and the Discovery Missions. It can also be used for analyzing surface reflection for solids such as Martian rock samples.

The LCWFTS sensor will provide a unique remote sensing and In-situ gas and rock/soil sensing capability to address a variety of NASA strategic objectives. Compared to the successful Shuttle-borne Atmospheric Trace Molecule Spectroscopy (ATMOS) FTS, the proposed EO-FTS system provides a new class of remote sensing instruments with over 3 orders of magnitude reduction in mass, volume, power, and telemetry rate. For instance, the ATMOS FTS has a volume of ~ 1 m^3, 250 kg, and 200 watts. The next version design still had a volume of ~0.25 m^3, mass of 20-25 kg,

and power of 50 watts. The proposed innovative EO-FTS has ultra-compact volume < 10^{-5} m^3, < 0.1 kg, ultra-low power < 0.06 Watt and zero power consumption when not measuring.

The low-mass, low-power, high-resolution characteristics, and adaptability to both in-situ and remote sensing environments of the proposed LCWFTS sensor will make it suitable for its inclusion in all spacecraft including flybys, orbiters, landers, as well as in the deployments of airplanes or balloons in planetary atmospheres, Earth orbiting telescopes and sample return missions to various solar System bodies. in-situ and/or remote sensing of gas measurements in the entire discovery mission. For example, operating in solar occultation mode, the LCWFTS spectrometer would cover the 1 to 2.5 micron region (10000 - 4000 cm^{-1}) with high signal-to-noise ratio and spectral resolution (0.25 cm^{-1}). Many atmospheric gases have their strongest absorption bands in the 1 to 2.5 micron region. These include NO, NO_2, CO_2, CO, OCS, N_2O, HNO_3, and N_2O_5, providing many opportunities for interesting science. For example, all the principle components of atmospheric Knox ($NO+NO_2$) and Nay ($NOx+HNO_3+2.N_2O_5+ClNO_3$) can be measured in this spectral region. These species are the major cause of stratospheric ozone destruction and require careful monitoring to gauge their response to climate change and changing amounts of stratospheric chlorine.

The LCWFTS gives the ability to make highly precise measurements of key tracers of atmospheric transport. Providing measurements of gases important for the photochemical regulation of 0, in the stratosphere over a wide range of conditions; using high quality tropospheric spectra to measure concentrations of H_2O, *0₃,* CO, HNO_3 and other species important for regulating OH; providing simultaneous observations of temperature, aerosol, ozone and water vapor for improved diagnosis of climate forcing; monitoring growth rates of greenhouse gases and precursors of 0, depleting catalysts; and detecting and monitoring industrial emissions of replacement compounds: fingerprinting the state of the atmosphere with high quality infrared spectra to preserve a record of gases which are growing in importance. This interferometer is insensitive to thermal and mechanical misalignment.

The key challenge to replacing the opto-mechanics has been realizing an EO material that provides sufficient voltage tunability over OPD. Typical EO crystals realize only a few microns of tunability of OPD, which is suitable for intensity modulators but hardly provides a viable replacement for opto-mechanics. This is especially true for FTS applications, where the magnitude of OPD is inversely related to the spectral resolution. In the next section we will discuss our liquid crystal-waveguide architecture that provides unprecedented voltage tunability over OPD.

2. CHIP-SCALE MONOLITHIC LC WAVEGUIDE FTS SYSTEM DESIGN

A detailed schematic of how a LC-waveguide may be used as an interferometer is depicted in Figure 1. The drawing is not to scale, but rather the waveguide core and cladding size is enhanced for visual clarity. The actual thickness of the waveguide lower cladding (≈8 μm) and core (≈1 μm) will be very small. The total length, however, will be on the order of 2-10 cm, depending on the desired range of OPD values. Specifically, the light to be analyzed is polarized 45° to the waveguide surface, and therefore equally couples into both the TE and TM modes. An LC waveguide section is used to vary the OPD between the TE and TM modes, which replaces the movable mirror. Finally, the two polarization-separate beams are recombined by means of a polarizer, which is aligned 45° with respect to the waveguide surface. To obtain the interferogram, one varies the OPD between TE and TM modes (via the LC waveguide), and records at the detectors the OPD dependent interference between them. All these elements will be integrated into a monolithic opto-block, thereby

eliminating all moving components and surmounting the foremost impediment to FTS miniaturization and cost reduction.

Depicted in Figure 1 is a divided upper electrode, providing two control voltages, one for large stroke adjustment to the TE/TM OPD, and the other for application of a high speed OPD dither (advantageous for noise reduction). Also, the two detector signals will be phase shifted with respect to one another. Auto-balancing circuits based on the two individual signals ratio-ed to their sum can be used to minimize the impact of source fluctuations. Also not shown are electrodes that are used for active waveguide dispersion compensation. This is the key, since optical waveguides possess significant geometric dispersion.

2.1 The Liquid Crystal Waveguide Architecture

As shown in Figure 2, the LC, instead of being used in a cell format, is used as an active cladding layer in waveguide architecture. In this way, the light skims along the surface of an LC layer. This *electro-evanescent* architecture circumvents limitations of traditional LC-optics: i) the light never crosses a transparent electrode, ii) the light only interacts with the well-behaved LC-surface layer via the evanescent field, and perhaps most importantly iii) the interaction length is now decoupled from the LC-layer thickness. In this way, the light interacts only with the surface layer of the LC cell, where the molecules are highly ordered (dramatically lower scattering loss) and they respond rapidly to both increases and decreases in electric field (surface mode effect greatly increases the speed, typical relaxation times for LC waveguides are on the order of *500 μsec*).

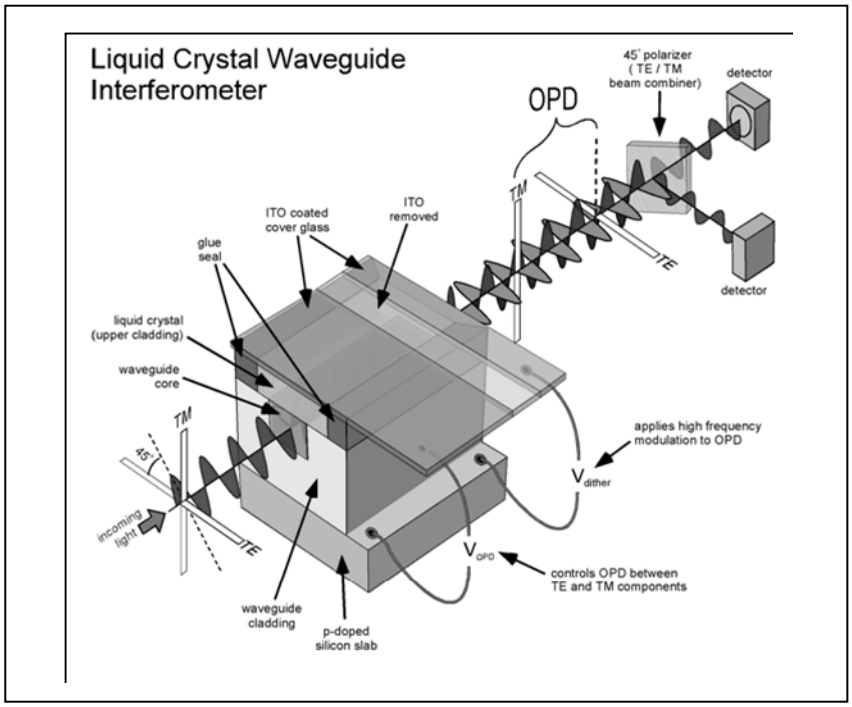

Figure 1: Schematic diagram of a liquid crystal waveguide based interferometer

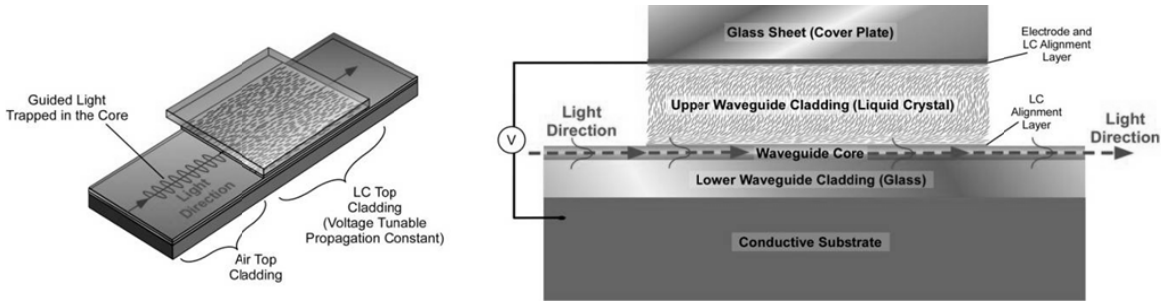

Figure 2 A) The basic geometry of an LC-waveguide. The light is confined to a core and the LC is an electro-optic upper cladding. As the index of refraction of the upper cladding is tuned the "effective index" of the guided mode is also tuned. B) A side view of a liquid crystal waveguide. In a slab waveguide the light is guided in the *x* dimension, but is free to propagate as Gaussian beams, sheets, or even 1D image in the plane.

2.2 Spectral Resolution

Similar to a conventional FTS, the spectral resolution, $\Delta\sigma$, of the proposed EO-FTS is related to the maximum optical path difference, Δx, or equivalently, the maximum time delay, $\delta_{max,}$ between the two interfering waves: $\Delta\delta = \frac{1}{2\pi OPD} = \frac{1}{2\pi d\left(n_o - n_e\right)}$. Our current LC-waveguide devices have greater than 1 mm of OPD, and we have designs for up to 1 or even 10 cm of OPD in a wrapped channel device. Thus the spectral resolution of <0.3 cm^{-1} (i.e. in sub-nanometer range at about 2μm IR spectral band) can in principle be realized.

2.3 Waveguide Development

The waveguide structures that are required for effective LC waveguide OPD control necessitate a tightly confined, high-contrast design. The core or guide layer must have an index that is higher than the LC cladding, i.e., $n_{core} > 1.75$. More specifically, a thin (< 1 μm), high index (n>1.8) core is optimal. The thin core layer pushes a significant fraction of the evanescent wave into the LC cladding, thereby increasing the total achievable electro-optic OPD. The higher index ensures sufficient intensity near the surface layer of the LC, thereby increasing speed and decreasing scattering losses. This need must be balanced with the pragmatic needs of: i) efficient coupling between the light source (be it fiber or other broadband light source), and ii) low loss operation. Our waveguide design provides very low waveguide losses of < 0.3 dB/cm and has integrated mode converters that provide very high coupling efficiencies of > 85%. Our waveguide are currently processed on 4 inch silicon wafers. An example of a typical LC-waveguide wafer run is shown in Figure 3. This wafer contains five individual devices.

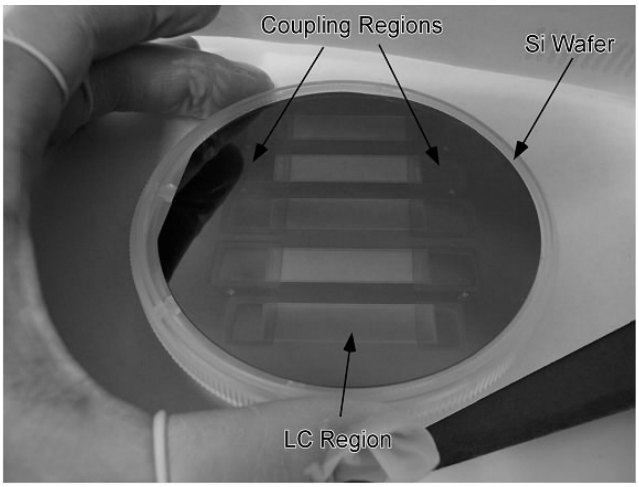

Figure 3. An image of one wafer from a waveguide foundry run. There are five dies on this one wafer. Visible in the picture are the in and out coupling regions (rectangles at the left and right) and the LC region (large rectangle in the middle. The LC interaction region is approximately 4 cm long.

Three different waveguide geometries have been explored for LC-Waveguide FTS devices. These three designs are shown in Figure 4. All three designs incorporate adiabatic mode-converters for efficient light source-to-waveguide couplings. All three designs also incorporate a micro-waveplate, which flips the TE and TM polarization half way through the waveguide, thereby setting the zero OPD point at zero voltage. In order to have a zero optical path difference point, the waveguide must be self compensated. Specifically, the significant geometric birefringence will make the zero voltage point correspond to a large OPD difference point. Stated differently, the TE polarization sees a different optical path than the TM polarization. In order to cancel this out, we insert a ½ waveplate mid-way through the device. This interchanges the TE and TM polarizations, which causes zero voltage on the LC to correspond to a zero optical path delay point. This is the same technique that renders planar waveguide telecom devices, such as arrayed waveguide gratings, polarization independent. While optical waveguides provide compactness and ruggedness, the single mode design also results in significant geometric dispersion, which can wash out the spectral resolution. Therefore, all of the designs also incorporate a dispersion compensation region. This dispersion compensation region is controlled with a separate electrode via a proprietary algorithm. At the cost of about 20% of the total OPD we have realized dispersion compensation over several 100 nm wide spectral windows.

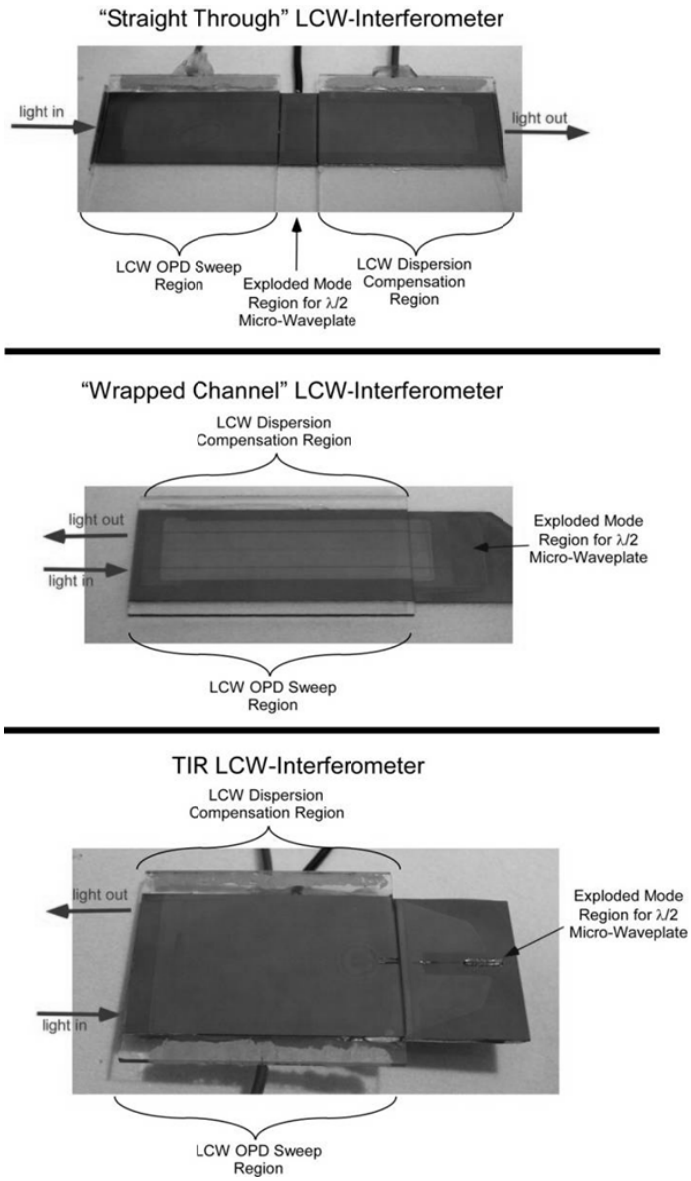

Figure 4 The above figure displays the three waveguide architectures that we are using for LC-Waveguide EO-FTS. All three of them have "exploded mode" input/output regions, wherein the guided beam is expanded to realize more efficient coupling. This exploded mode region is also used for insertion of the half waveplate, which is required for setting of the zero OPD point. The middle figure shows a channel waveguide design. The bottom figure shows a TIR design, with the half waveplate inserted. The top design is a straight-through slab-waveguide approach, with no beam redirection. This design is optically simpler, but the total path length is cut in half, which limits the resolution of the device.

2.4 Broadband Light Source

Key to a complete FTS sensor system is the appropriate broadband light source. The LC waveguide interferometer requires a high spatial coherence, i.e., all of the light must be confined to the guided mode. In addition to the high *spatial* coherence requirement, low *temporal* coherence is sought, for broadband spectral coverage. While numerous possibilities exist (e.g., halogen lamps, heated elements, LEDs), an especially attractive, very compact and low noise option is provided by super luminescent diodes (SLDs). SLDs with single-mode broadband powers of 10-20 mw are now commercially available. As an example, companies such as Superlum Diodes, Ltd. provide arrays of

five SLDs to provide extended spectral coverage. For greater spectral coverage, this array could incorporate as many SLDs as desired; examples of 32 element diode arrays are given in the literature.

3. PROTOTYPE LCWFTS CONSTRUCTION AND TESTING

3.1 LCWFTS System Integration and Results

A LC waveguide, operational in the near-IR band, has been built and tested. The LC waveguide and its close-up view showing the dispersion compensation approach is shown in Figure 5.

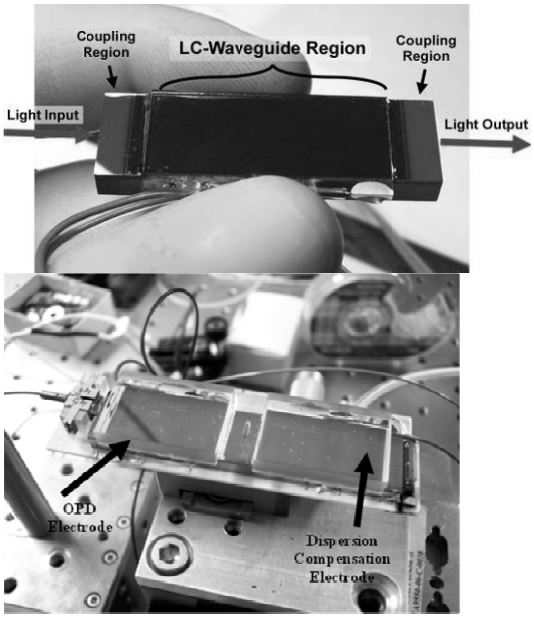

Figure 5: A. The prototype LC-Waveguide for operation in the near-IR. B. close-up view of a LC Waveguide with a dispersion compensation approach.

We have accomplished a LCWFTS breadboard include the waveguide, the SLD light source and the driving electronics. A picture of this LCWFTS is shown in Figure 6.

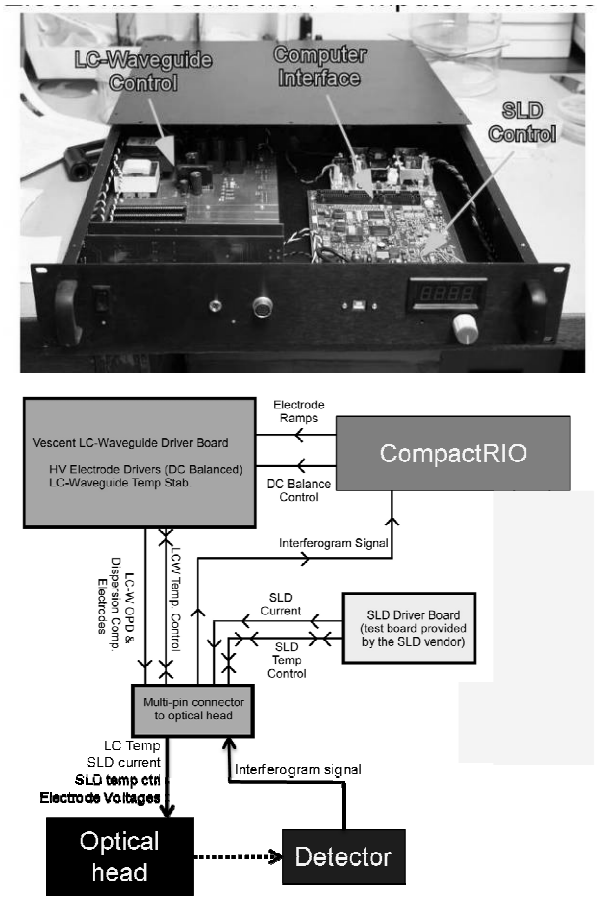

Figure 6. A. A picture of the LCWFTS electronics driver (the LC waveguide optics head is placed separately outside the box. B. The schematic diagram of the electronic control functional block diagram of the LCWFTS driver.

The overall LCWFTS breadboard setup picture is shown in Figure 7.

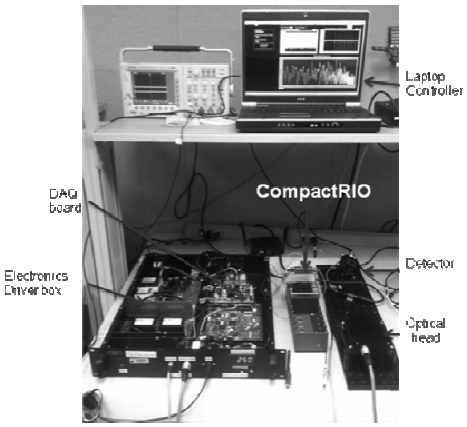

Figure 7. Picture of the overall LCWFTS system laboratory setup.

3.2 Experimental Results

We have performed experimental investigation on the system spectral impulse response of the LCWFTS. First, waveguide interferometer output interferogram of the SLD light source and the reconstructed spectral waveform is shown in Figure 8.

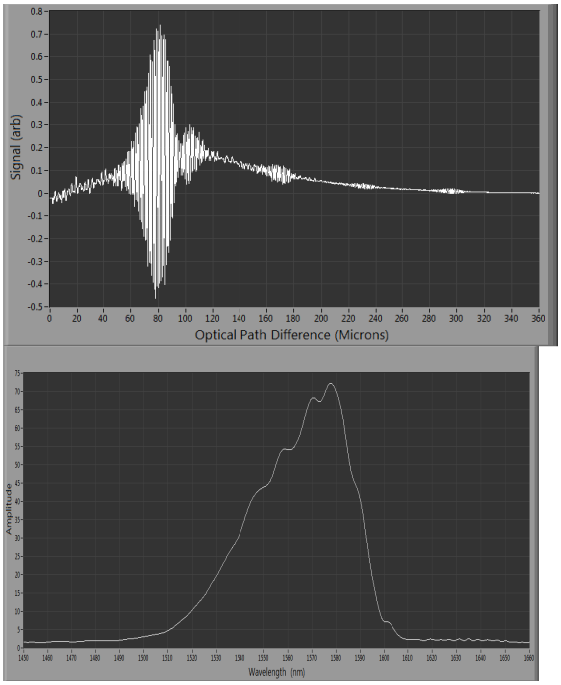

Figure 8. A. The LCWFTS output interferogram of the input SLD light source emission. B. The reconstructed (Inverse FFT) spectral waveform of the light source.

In a second experimental investigation, we have placed a narrow spectral band notched filter bandwidth into the input light path of the LCWFTS. The measured output interferogram and the corresponding reconstructed spectral waveform is shown in Figure 9. It is noted that the central wavelength (CWL) is 1550 nm and the full-width half-maxi- mum (FWHM) is 12 nm. The throughput waveform shown in Figure 9b matched perfectly well with the CWL of the notch filter. The measured bandwidth is 15 nm. This means that the spectral resolution of the LCWFTS is about 3-4 nm that also matches with the design.

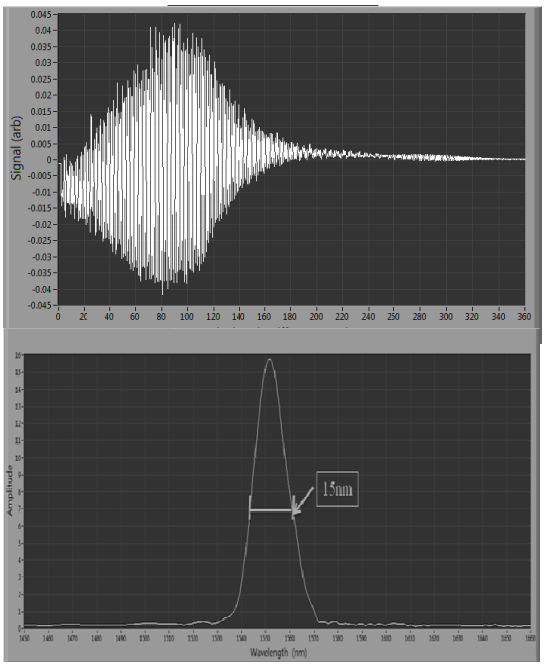

Figure 9. A. Output interferogram with a notch filter inserted into the light path of the LCWFTS. B. The reconstructed spectral waveform.

We have also experimentally evaluated the effectiveness of the dispersion compensation. We have measured the output spectral using a single frequency tunable laser source. As shown in Figure 10 A (left), without turning the dispersion compensation electrode, the spectral waveform begins to deviate from a sharp impulse as the wavelength is incrementally tuned upward. On the other hand, with applying compensation driving signal to the waveguide, the output spectral waveform remains sharp throughout the tuning range of the tunable laser source. In Figure 10 B, (right), the FWHM of the LCWFTS remains constant with dispersion compensation. However, the FWHM start to broaden as it is measure away from the calibration wavelength.

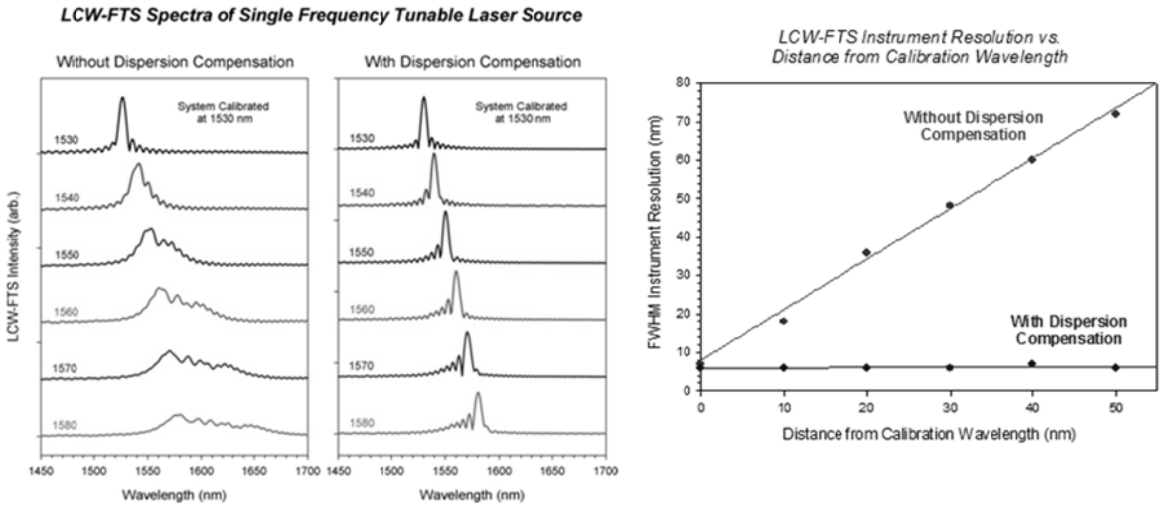

4. SUMMARY

A prototype LCWFTS sensor breadboard was designed and built and tested. The prototype spectrometer is a fully packaged system with a near-IR spectral range from about 1450-1700 nm, with a spectral resolution of about 4 nm. The integrated light source is a super-luminescent diode. The system is designed for in-situ analysis, though both remote and reflectance systems are possible. These results of our experimentally investigations demonstrated the feasibility of the LC waveguide based non-mechanical FTS systems. We have developed an effective dispersion compensation mechanism by utilizing a double electrode design to drive the waveguide. Furthermore, engineering improvements to the system will improve the resolution to 0.5 nm and possibly even 0.1 nm, all in a small, low power, and non-mechanical package.

5. ACKNOWLEDGMENTS

The research described in this paper was supported by contracts from both the National Aeronautics and Space Administration and the National Oceanic and Atmospheric Administration.

6. REFERENCES

1. S. P. Davis, M. C. Abrams, and J. W. Brault, Fourier Transform Spectrometry (Academic Press, 2001).
2. http://atmos.jpl.nasa.gov/atmos/pub.list.html.
3. T.-H. Chao, H. Zhou, X. Xia, and S. Serati, "Near IR electro-optic Imaging Fourier Transform Spectrometer," Optical Pattern Recognition XVI, Proceedings of SPIE 5816, 163-171 (2005).
4. Tien-Hsin Chao, Thomas T. Lu, Scott R. Davis, et al. "Compact liquid crystal waveguide based Fourier transform spectrometer for in-situ and remote gas and chemical sensing, " Proceedings of SPIE 6977 (2008)
5. I.-C. Khoo, and S.-T. Wu, Optics and nonlinear optics of liquid crystals (World Scientific Publishing, 1993).
6. M. Anderson, S. Rommel, and S. Davis, "Liquid Crystal Waveguide for Dynamically Controlling Polarized Light," USPTO, ed. (Vescent Photonics, USA, 2005).
7. M. Anderson, S. Rommel, and S. Davis, "Liquid Crystal Waveguide Having Electric Field Oriented for Controlling Light," USPTO, ed. (Vescent Photonics, USA, 2006).
8. M. Anderson, S. Rommel, and S. Davis, "Liquid Crystal Waveguide Having Two or More Control Voltages for Controlling Polarized Light," USPTO, ed. (Vescent Photonics, USA, 2006).
9. J. Malinen, M. Kansakoski, R. Rikola, and C. G. Eddison, "LED-based NIR spectrometer module for hand-held and process analyser applications," Sensors and Actuators B 51, 220 (1998).